genes

MDPI

Article

LTBP3 Frameshift Variant in British Shorthair Cats with Complex Skeletal Dysplasia

Gabriela Rudd Garces [1,2,†], Anna Knebel [3,†], Kirsten Hülskötter [4,5,†], Vidhya Jagannathan [1], Theresa Störk [4], Marion Hewicker-Trautwein [4], Tosso Leeb [1,*,‡] and Holger A. Volk [3,5,‡]

1 Institute of Genetics, Vetsuisse Faculty, University of Bern, 3001 Bern, Switzerland; gabriela.ruddgarces@vetsuisse.unibe.ch (G.R.G.); vidhya.jagannathan@vetsuisse.unibe.ch (V.J.)
2 Institute of Veterinary Genetics "Ing. Fernando Noel Dulout", National University of La Plata, La Plata 1900, Argentina
3 Department of Small Animal Medicine and Surgery, University of Veterinary Medicine Hannover, 30559 Hannover, Germany; anna.knebel@tiho-hannover.de (A.K.); holger.volk@tiho-hannover.de (H.A.V.)
4 Department of Pathology, University of Veterinary Medicine Hannover, 30559 Hannover, Germany; kirsten.huelskoetter@tiho-hannover.de (K.H.); theresa.stoerk@tiho-hannover.de (T.S.); marion.hewicker-trautwein@tiho-hannover.de (M.H.-T.)
5 Center for Systems Neuroscience Hannover (ZSN), 30559 Hannover, Germany
* Correspondence: tosso.leeb@vetsuisse.unibe.ch; Tel.: +41-31-684-23-26
† These authors contributed equally to this work.
‡ These authors are senior authors.

Abstract: We investigated a highly inbred family of British Shorthair cats in which two offspring were affected by deteriorating paraparesis due to complex skeletal malformations. Radiographs of both affected kittens revealed vertebral deformations with marked stenosis of the vertebral canal from T11 to L3. Additionally, compression of the spinal cord, cerebellar herniation, coprostasis and hypogangliosis were found. The pedigree suggested monogenic autosomal recessive inheritance of the trait. We sequenced the genome of an affected kitten and compared the data to 62 control genomes. This search yielded 55 private protein-changing variants of which only one was located in a likely functional candidate gene, *LTBP3*, encoding latent transforming growth factor β binding protein 3. This variant, c.158delG or p.(Gly53Alafs*16), represents a 1 bp frameshift deletion predicted to truncate 95% of the open reading frame. LTBP3 is a known key regulator of transforming growth factor β (TGF-β) and is involved in bone morphogenesis and remodeling. Genotypes at the *LTBP3*:c.158delG variant perfectly co-segregated with the phenotype in the investigated family. The available experimental data together with current knowledge on *LTBP3* variants and their functional impact in human patients and mice suggest *LTBP3*:c.158delG as a candidate causative variant for the observed skeletal malformations in British Shorthair cats. To the best of our knowledge, this study represents the first report of *LTBP3*-related complex skeletal dysplasia in domestic animals.

Keywords: *Felis catus*; skeletal dysplasia; bone; development; whole genome sequence; precision medicine; animal model

check for updates

Citation: Rudd Garces, G.; Knebel, A.; Hülskötter, K.; Jagannathan, V.; Störk, T.; Hewicker-Trautwein, M.; Leeb, T.; Volk, H.A. *LTBP3* Frameshift Variant in British Shorthair Cats with Complex Skeletal Dysplasia. *Genes* **2021**, *12*, 1923. https://doi.org/10.3390/genes12121923

Academic Editor: Anna V. Kukekova

Received: 22 October 2021
Accepted: 28 November 2021
Published: 29 November 2021

Publisher's Note: MDPI stays neutral with regard to jurisdictional claims in published maps and institutional affiliations.

Copyright: © 2021 by the authors. Licensee MDPI, Basel, Switzerland. This article is an open access article distributed under the terms and conditions of the Creative Commons Attribution (CC BY) license (https://creativecommons.org/licenses/by/4.0/).

source: https://doi.org/10.48350/161736 | downloaded: 12.10.2024

1. Introduction

Skeletal dysplasias are a diverse group of phenotypes related to bone and cartilage development. Due to their heterogeneity, classification may be based on the genetic cause, lethality or involvement of similar skeletal parts [1]. Pathogenic variants affecting 437 different genes have been identified in human bone disorders [2].

In domestic animals, various skeletal dysplasias are known. In some instances, the selection for desired anatomical attributes during animal breeding has led to the genetic fixation of skeletal malformations, which have become breed standards. However, most skeletal dysplasias in domestic animals are considered diseases [3–5].

In cats, only a few skeletal dysplasias have been characterized at the molecular level. Osteochondrodysplasia in Scottish fold cats is caused by a missense variant in the *TRPV4* gene (000319-9685) [6,7]. A form of chondrodysplasia that represents the breed standard in short-legged Munchkin cats is caused by a large deletion within the *UGDH* gene encoding UDP-glucose 6-dehydrogenase (OMIA 000187-9685) [8,9]. The extreme brachycephaly in Burmese cats is at least partly due to a 12 bp deletion in the *ALX1* gene encoding the ALX homeobox 1 protein (OMIA 001551-9685) [10]. Polydactyly in cats is caused by non-coding SNVs in a regulatory region of the *SHH* gene encoding sonic hedgehog, a developmental morphogen (OMIA 000810-9685) [11]. A missense variant in the *ACVR1* gene encoding activin A receptor type I was reported in domestic shorthair cats with fibrodysplasia ossificans and secondary skeletal malformations (OMIA 000388-9685) [12].

There are several cat breeds, such as Pixie Bob, Kurilian Bobtail, American Bobcat, Japanese Bobcat and Manx, with shortened or kinked tails. Causative variants for these spinal malformations have been identified in the *TBXT* (OMIA 000975-9685) [13] and *HES7* genes (OMIA 001987-9685) [14,15].

The present study was initiated after a breeder reported two British Shorthair littermate kittens with severe skeletal deformations. The goal of this study was to characterize the clinical and radiological phenotype and to investigate a possible underlying causative genetic defect.

2. Materials and Methods

2.1. Animals

This study investigated two British Shorthair kittens affected by complex skeletal malformations. The affected cats, one male and one female, were littermates. We additionally obtained samples from both parents, six unrelated British Shorthair cats and 90 cats of other breeds.

2.2. Clinical Examinations

A general clinical and neurological examination was performed on the two affected kittens and their parents. Radiographs of the thorax and abdomen were obtained of both kittens in latero-lateral and ventro-dorsal projections. Post mortem computed tomography (CT, Philips Brilliance CT, Philips Medical Systems, Cleveland, OH, USA) and magnet resonance imaging (MRI, Phillips Achieva 3 Tesla MRI Scanner, Phillips Medical Systems) were performed on the euthanized male kitten (full body scan). Sagittal and transverse CT images and T1-weighted as well as T2-weighted images (MRI) were obtained. Cerebrospinal fluid (CSF) was taken post mortem by suboccipital puncture and analyzed.

2.3. Necropsy and Histopathological Examination

A full necropsy was performed of the male kitten after standard protocol. Tissue samples of all organs were taken and fixed in 10% neutral-buffered formalin for 24 h. Frozen tissue samples from the liver, pinna and skin were obtained for genetic analysis. Formalin fixed tissues were trimmed and embedded in paraffin, prior to routine histology, Luxol-Fast-Blue staining and immunohistochemistry on 2–3 µm thick tissue sections.

2.4. Immunohistochemistry

For immunohistochemistry, the tissue sections were deparaffinized and rehydrated by immersion in Roticlear (Carl Roth, A538.1, Karlsruhe, Germany) followed by isopropanol and 96% ethanol for 2 min each. Endogenous peroxidase was blocked with a solution of 85% ethanol with 0.5% H_2O_2 for 30 min at room temperature, prior to antigen retrieval by boiling for 20 min in 10 mM citrate buffer (pH 6) in the microwave. Unspecific bindings were blocked with goat serum (dilution 1:5) for 20 min. Primary antibodies (anti-Alzheimer precursor protein A4, a.a. 66–81 of APP (N-terminus), clone 22C11, Merck Millipore, Darmstadt, Germany; MAB348; dilution 1:2000; anti-pan-neuronal neurofilament marker mouse mAb SMI-311, Merck Millipore; NE1017, dilution 1:1000) were incubated at 4 °C

overnight. The secondary antibody (biotinylated goat anti-mouse IgG, Vector BA9200; dilution 1:200) was incubated for 1.5 h, and positive signals were visualized using avidin–biotin–peroxidase complex (ABC Kit, Vectastain, PK6100, Vector Laboratories, Burlingame, CA, U.S.A.) and 0.1 g 3,3′-diaminobenzidine-tetrahydrochloride hydrate (DAB) in 200 mL PBS with 0.03% H_2O_2. The tissues were dehydrated in alcohol and mounted with Roti-Histokit II (Carl Roth, Karlsruhe, Germany, T160.1).

2.5. DNA Isolation

Genomic DNA was isolated from 500 µL EDTA blood samples of the cats in the study with the Maxwell RSC Whole Blood Kit, using a Maxwell RSC instrument (Promega, Dübendorf, Switzerland).

2.6. Whole Genome Sequencing of an Affected Kitten

An Illumina TruSeq PCR-free DNA library with ~400 bp insert size of an affected British Shorthair kitten was prepared. We collected 296 million 2 × 150 bp paired-end reads on a NovaSeq 6000 instrument (32.3× coverage). The reads were mapped to the Felis_catus_9.0 cat reference genome assembly as previously described [16]. The sequence data were deposited under study accession PRJEB7401 and sample accession SAMEA8609185 at the European Nucleotide Archive.

2.7. Variant Calling

Variant calling was performed as described [16]. To predict the functional effects of the called variants, SnpEff [17] software together with NCBI annotation release 104 for the Felis_catus_9.0 genome reference assembly was used. For variant filtering, we used 62 control genomes (Table S1). We employed a hard filtering approach to identify variants at which the affected cat was homozygous for the alternate allele (1/1) while 62 control genomes were either homozygous for the reference allele (0/0) or had a missing genotype call (./.). The output of the variant filtering is given in Table S2.

2.8. Gene Analysis

We used the Felis_catus_9.0 cat reference genome assembly and NCBI annotation release 104. Numbering within the feline *LTBP3* gene corresponds to the NCBI RefSeq accession numbers XM_023240055.1 (mRNA) and XP_023095823.1 (protein).

2.9. Targeted Genotyping and Sanger Sequencing

The *LTBP3*:c.158delG variant was genotyped by direct Sanger sequencing of PCR amplicons. A 557 bp PCR product was amplified from genomic DNA using AmpliTaq-Gold360Mastermix (Thermo Fisher Scientific, Waltham, MA, U.S.A.) together with primers 5′-CGCTTCCTCTGTTCCTCTCC-3′ (Primer F) and 5′-AGACCCTACCCCACCAGGTA-3′ (Primer R). A 5200 Fragment Analyzer was used for the quality control of PCR products (Agilent, Santa Clara, CA, USA). After treatment with shrimp alkaline phosphatase and exonuclease I, PRC amplicons were sequenced on an ABI 3730 DNA Analyzer (Thermo Fisher Scientific). Sanger sequences were analyzed using the Sequencher 5.1 software (GeneCodes, Ann Arbor, MI, USA). The *CAPN1*:c.1295G>A variant was genotyped with the same methodology and these primers for the PCR amplification: 5′-CCTCCTACAGCCACCTT CTG-3′ (Primer F) and 5′- GTTCGTCGTGATCGTGTGAT-3′ (Primer R). Genotypes at the *CAPN1* and *LTBP3* variants were also extracted from the gvcf-file of the 99 Lives consortium (version with 340 cats) as described [8].

3. Results

3.1. Phenotype Description

Two British Shorthair littermates, one male and one female, with deteriorating paraparesis and their unaffected parents were investigated. The litter consisted of two affected and three non-affected kittens. The breeder noticed first signs of hind limb paraparesis

in the affected kittens at 8 weeks of age. At 10 weeks of age, a clinical and neurological examination demonstrated lordosis and scoliosis, T3-L3 myelopathy and reduced motility of the intestine. Both kittens showed ambulatory paraparesis (Video S1). Hematology and cerebrospinal fluid analyses were inconspicuous. Radiography demonstrated severe vertebral column deformations and marked coprostasis (Figures 1 and S1). Due to the severity of the clinical signs, the kittens were euthanized.

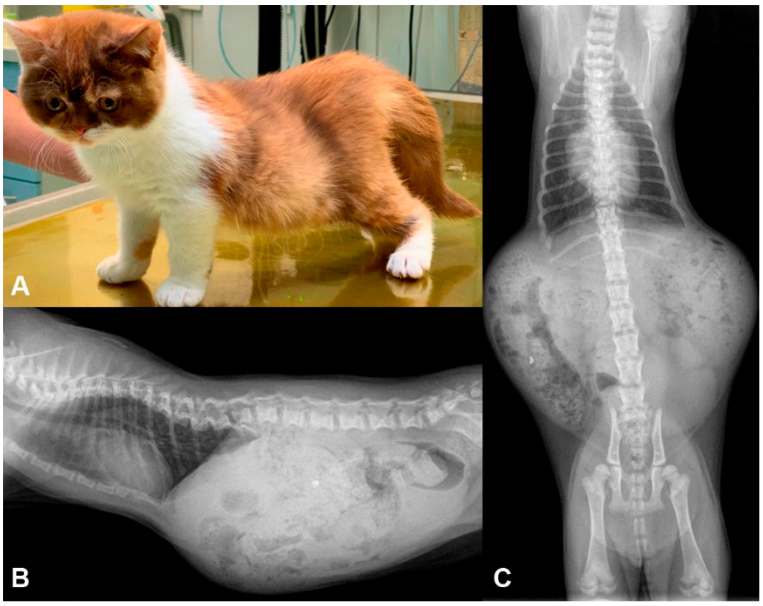

Figure 1. Clinical phenotype. (**A**) Photograph of the affected female kitten. (**B**) Radiograph in latero-lateral projection of the female kitten. (**C**) Radiograph in ventro-dorsal projection of the female kitten. Note the lordosis of this kitten, the malformation of the vertebral column within the thoracic region and the enlarged abdomen due to coprostasis.

The post mortem examination of the male affected kitten by CT and MRI confirmed the deformation of multiple thoracic vertebral bodies. From T11 to L3, there was moderate to marked stenosis of the vertebral canal (lateral narrowing) as well as secondary compression of the spinal cord tissue, which could have led to the T3-L3 myelopathy. The MRI images also revealed an ascending and descending dilation of the central canal of the spinal cord (hydromyelia) and cerebellar herniation (Figure 2).

At necropsy, the multiple skeletal malformations with shortened legs, deviations of the spine and flattening of the occiput with narrowing of the caudal cranial fossa were corroborated. Parts of the caudal cerebellum and vermis were irreversibly dislocated into the foramen magnum with prominent indented deformation (Figure S2). The thoracic vertebral column showed a mild dorsal bend (kyphosis) with a following, moderate, ventral deformation (lordosis) and a minor lateral deviation (scoliosis) accompanied by a focal stenosis of the spinal canal at T11–12. The ventral cortical laminar bone showed an increased density and thickening up to 1 mm and the woven bone of the vertebral body was irregularly arranged (Figure S3). The ventral cortical laminar bone of the vertebral bodies showed an increased density and thickening up to 1 mm and the woven bone of the vertebral body and femur was irregularly arranged (Figures S3 and S4). Except for the compression of the caudal cerebellum, the histopathological examination of the brain was unremarkable. The compression of the thoracic spinal cord was associated with myelin damage accentuated in the dorso-lateral funiculi but also seen in the ventral aspects with dilation of myelin sheaths, axonal swelling (spheroid formation) and degeneration (Figure S5). The coprostasis was caused by annular constrictions of the colon and rectum with distention of anterior aspects (Figure S6). The constricted areas of the intestine showed a marked hypertrophy of the muscle layer (Figure S7) with loss of neurons in

the submucosal (Meissner) and myenteric (Auerbach) plexus (hypoganglionosis). The thickening of the intestinal wall was accompanied by proliferation of vascularized fibrous connective tissue (granulation tissue) in the submucosa, between the muscle layers as well as the subserosa. Despite the loss of neurons, there was an excessive proliferation of nerve fibers interwoven into the granulation tissue and crossing the muscular layers (Figure S8).

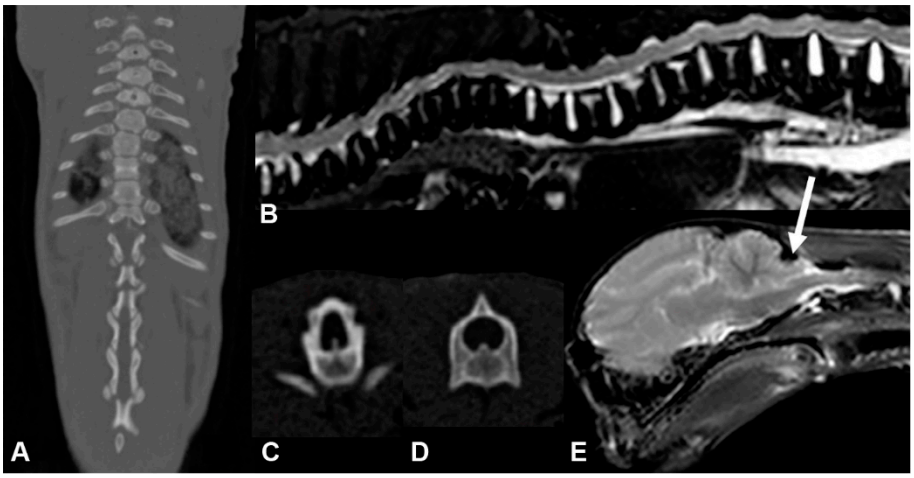

Figure 2. CT/MRI images of the affected male kitten. (**A**) CT image of the thoracic region in dorsal view. (**B**) T2-weighted sagittal MRI image of the vertebral column. (**C**) Transverse CT image of the vertebral body at the level of Th13. (**D**) Transverse CT image of the vertebral body at the level of L5. (**E**) T2-weighted sagittal MRI image of the brain with cerebellar herniation (white arrow).

3.2. Genetic Analysis

The two affected kittens came from a highly inbred family. The sire and dam were half siblings. The pedigree relationships were suggestive for a monogenic autosomal recessive mode of inheritance of the trait (Figure 3).

The genome of the male affected kitten was sequenced at 32.3× coverage and variants were called with respect to the Felis_catus_9.0 reference genome assembly. Subsequently, we searched for private homozygous variants in the genome of the affected cat that were not present in the 62 control genomes. The variant calling pipeline detected 55 private protein-changing variants in 28 genes (Table 1).

Table 1. Homozygous variants detected by whole genome re-sequencing of an affected cat.

Filtering Step	Variants
Variants in whole genome	5,759,180
Private variants (absent from 62 control genomes)	7398
Protein-changing private variants	55

We then prioritized the 55 protein-changing variants according to the functional knowledge on the altered genes. Two closely linked variants on chromosome D1 affected genes with potential relevance for the observed phenotype. The affected cat had a missense variant in the *CAPN1* gene, XP_023095818.1:p.(Arg432His), and a frameshift deletion in the *LTBP3* gene encoding the latent transforming growth factor β binding protein 3 (Figure 4). The *LTBP3* variant was considered the most likely cause for the observed phenotype (see discussion). This candidate variant, a 1 bp deletion in the first exon of *LTBP3*, can be designated as ChrD1:110,690,432delC (Felis_catus_9.0 assembly). It is a frameshift variant, XM_023240055.1:c.158delG, predicted to truncate 95% of the open reading frame, XP_023095823.1:p.(Gly53Alafs*16).

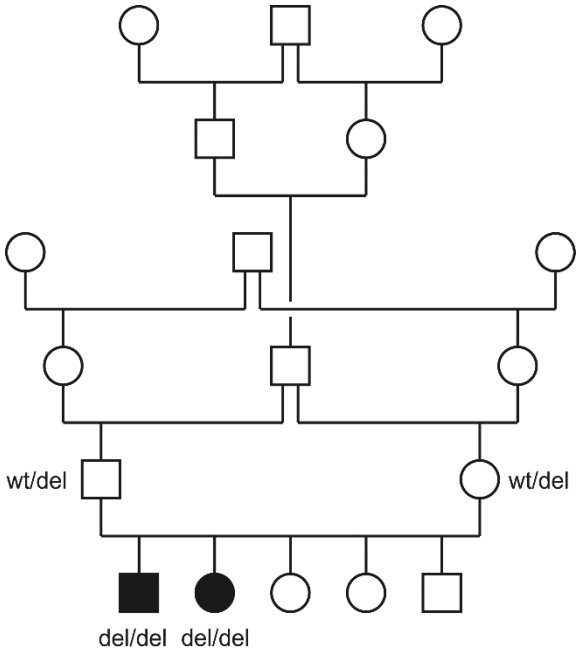

Figure 3. Pedigree of the investigated British Shorthair family. Filled symbols indicate affected cats and open symbols indicate non-affected cats. Squares and circles represent males and females, respectively. Note the multiple inbreeding loops in this pedigree. Genotypes at the *LTBP3*:c.158del variant are given for cats from which the samples were available.

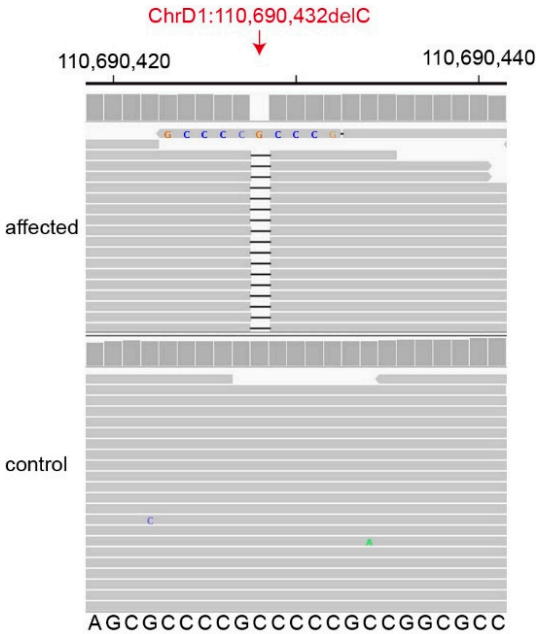

Figure 4. Details of the *LTBP3*:c.158delG, p.(Gly53Alafs*16) variant. Integrative Genomics Viewer (IGV) screenshot showing the short-read alignments of the affected kitten and a control cat at the position of the deletion, which affects the coding part of the first exon. Note that in the IGV screenshot, base 110,690,428 is deleted, which represents the first possible position of the deletion. Taking into consideration the 3′-rule of HGVS nomenclature, the correct variant designation is ChrD1:110,690,432delC (Felis_catus_9.0 assembly).

We genotyped the *CAPN1* and *LTBP3* variants in the parents and the two affected littermates by Sanger sequencing. Both cases were homozygous for the mutant allele while the parents were heterozygous carriers. The segregation of the genotypes was compatible

with a monogenic autosomal recessive mode of inheritance. We also genotyped the two variants in 6 additional unrelated British Shorthair cats and 90 other genetically diverse cats. The mutant *CAPN1* and *LTBP3* alleles were absent from all the tested unrelated control cats (Table 2).

Table 2. Association of the genotypes at the *CAPN1* and *LTBP3* variants with the skeletal malformation.

Phenotype	*CAPN1*:c.1295G>A	*LTBP3*:c.158delG
Cases (n = 2)	A/A	del/del
Non-affected parents (n = 2)	G/A	wt/del
Non-affected British Shorthair cats (n = 6)	G/G	wt/wt
Random-bred cats and cats from other breeds (n = 90)	G/G	wt/wt

We finally extracted the genotypes at these two variants from 340 cat genomes of the 99 Lives Consortium. A total of 8 random-bred cats of the 340 cats carried the mutant *CAPN1* allele in a heterozygous state (allele frequency 1.2%), while none of the cats carried the mutant *LTBP3* allele.

4. Discussion

The present article describes the clinical and pathological findings of a new form of inherited skeletal dysplasia in two full sibling British Shorthair cats.

The detected skull malformation with indentation of the occipital bone and cerebellar herniation through the foramen magnum resembles the "Chiari-like malformation" of dogs [18–21]. As the histopathological examination of the cerebellum and brain stem was unremarkable and there were no signs of syringomyelia, it is likely that the ataxia in the presented kittens was not solely caused by the protrusion of the cerebellar vermis into the foramen magnum. More likely, the reported ataxia and weakness of hind limbs were the consequence of the degenerative processes in the thoracic spinal cord and due to spinal cord compression.

The density and orientation of the trabecular bone was abnormal, which could indicate problems with the physiological remodeling. Nonetheless, it is unclear if a possible impairment of bone remodeling is fully responsible for the skeletal deformations or if the abnormal body posture and gait of the kittens may have contributed to the aberrant orientation of trabecular bone.

Histopathological examination of the colon revealed a segmental, distal hypoganglionosis with hypertrophy of the musculature and nerve fibers, as well as chronic inflammation with the formation of granulation tissue. These findings resemble another case report of a kitten with congenital colonic hypoganglionosis [22] and the diagnostic criteria for the congenital megacolon, known as "Hirschsprung's disease" (HSCD) in humans [23]. The aganglionosis, seen in HSCD, is occasionally seen together with complex skeletal malformations [24] and could be caused by impaired migration and differentiation of neural stem cells from the neural crest [25]. However, in the studied cats, a primary neural crest defect seems unlikely. Our data suggest that the skeletal dysplasia caused secondary neuronal damage during pre- and postnatal development.

The genetic analysis revealed two tightly linked private protein-changing variants in the affected cat, a missense variant in *CAPN1* and a frameshift variant in *LTBP3*. *CAPN1* loss-of-function variants lead to autosomal recessive spastic paraplegia-76 in human patients [26] and spinocerebellar ataxia in Parson Russell Terriers [27]. It is unclear whether the *CAPN1*:p.Arg432His variant in the British Shorthair cat has any impact on calpain 1 function. Even if calpain 1 function in the affected cat was compromised, this would not explain the skeletal phenotype, but it may have possibly contributed to the neurological phenotype. As the mutant *CAPN1* allele was also present at a low frequency in the 99 Lives dataset, we consider a major functional impact of the *CAPN1* variant unlikely.

The *LTBP3*:c.158delG variant represents an excellent candidate causative variant for the skeletal phenotype. *LTBP3* encodes the latent transforming growth factor β binding

protein 3, which is highly expressed in the heart, lungs, and bones and has a known role in TGF-β signaling and bone homeostasis [28,29].

TGF-β with its three isoforms encoded by the *TGFB1*, *TGFB2* and *TGFB3* genes is an important cytokine involved in the growth and remodeling of bones and many other tissues [30]. TGF-β is synthesized as an inactive precursor molecule that is proteolytically cleaved in the endoplasmic reticulum to yield a TGF-β homodimer in complex with the latency associated peptide (LAP). This complex is termed small latent complex (SLC). LTBP3 and other members of the LTBP family bind to the SLC, form covalent disulfide bonds with the LAP [31] and yield the large latent complex (LLC). The LLC is further processed in the Golgi apparatus, exported from the cell, and finally deposited in the extracellular matrix [32]. Activation of TGF-β signaling requires degradation of the LAP or release of active TGF-β homodimers from the LLC by other mechanisms [29–31]. LTBP3 and other members of the LTBP family are required to mediate the export and anchoring of the LLC to the extracellular matrix. LTBP3 deficiency reduces TGF-β activation and, therefore, may diminish associated cell proliferation and osteogenic differentiation [33]. Deregulation of the TGF-β signaling pathway is associated with numerous human diseases with prominent involvement of the skeletal system [34].

Human patients with bi-allelic loss-of-function variants in *LTBP3* develop dental anomalies and short stature (DASS, OMIM #601216). DASS is inherited as an autosomal recessive trait and clinical features may include oligodontia, amelogenesis imperfecta, short stature, brachyolmia and scoliosis, platyspondyly, cone-shaped epiphysis, undertubulation of the long bones, and in some instances also cardiac defects [35–39].

Other *LTBP3* variants cause an autosomal dominant phenotype in humans, termed geleophysic dysplasia 3 (GPHYSD3, OMIM #617809). The phenotype of GPHYSD3 overlaps with DASS and involves short stature, brachydactyly, restricted movements in the elbow and wrist joints, and dysmorphic facial features [40,41].

Ltbp3$^{-/-}$ homozygous null mice had shorter endochondral bones and smaller overall size compared to their wild-type littermates. *Ltbp3*$^{-/-}$ mice also developed craniofacial malformations and curvature of thoracic/cervical vertebrae (scoliosis). In addition, histological examination of *Ltbp3*$^{-/-}$ skeletons revealed an increase in bone mass and persistence of cartilage remnants in trabecular bone, thus indicating a defect in bone resorption. A lack of Ltbp3 was suggested to result in decreased levels of TGF-β in bone and cartilage, which disrupts osteoclast function and bone turnover [42–44].

The *LTBP3* frameshift variant, c.158delG, p.(Gly53Alafs*16), in the British Shorthair cats of this study leads to a very early premature stop codon. We consider it, therefore, unlikely that any functional LTBP3 protein is expressed in homozygous mutant cats. Unfortunately, an experimental confirmation on the transcript or protein level could not be performed, as no suitable tissue samples were available. However, the genotype–phenotype co-segregation in the family together with the existing knowledge on the functional effect of *LTBP3* variants in humans and mice with skeletal dysplasia phenotypes support *LTBP3*:c.158delG as a candidate causative variant for the skeletal phenotype in the affected British Shorthair cats.

5. Conclusions

In summary, we characterized a new, recessively inherited form of skeletal dysplasia in British Shorthair cats and identified a frameshift variant in the *LTBP3* gene, c.158delG, as a candidate causative variant. Our data enable genetic testing to avoid the unintentional breeding of further affected cats and provide a potential spontaneous large animal model for *LTBP3*-related skeletal dysplasia.

Supplementary Materials: The following are available online at https://www.mdpi.com/article/10.3390/genes12121923/s1, Figure S1: Photograph of the male affected kitten. Figure S2: Male affected kitten, dorso-caudal cerebrum and cerebellum. Figure S3: Male affected kitten, longitudinal cut of vertebral column with ribs. Figure S4: Longitudinal cut of thoracic vertebral column of the (A) male affected kitten and (B) an unaffected, age-matched kitten. Femur head of the (C) male

affected kitten and (D) unaffected control. Figure S5: Male affected kitten, thoracic spinal cord, dorso-lateral funiculus. Figure S6: Male affected kitten, colon and rectum. Figure S7: Male affected kitten, colon. Figure S8: Male affected kitten, hypoganglionosis, colon. Table S1: Accession numbers of 63 cat genome sequences. Table S2: Private variants in the genome of the sequenced affected British Shorthair cat. Video S1: Clinical phenotype of the female affected kitten.

Author Contributions: Conceptualization, T.L. and H.A.V.; investigation, G.R.G., A.K. and K.H.; data curation, V.J.; writing—original draft preparation, G.R.G., A.K., K.H. and T.L.; writing—review and editing, G.R.G., A.K., K.H., V.J., T.S., M.H.-T., T.L. and H.A.V.; visualization, G.R.G., A.K. and K.H.; supervision, M.H.-T., T.L. and H.A.V. All authors have read and agreed to the published version of the manuscript.

Funding: G.R.G. received a Swiss Government Excellence Scholarship, which enabled her to conduct this research.

Institutional Review Board Statement: All animal procedures were performed according to local regulations. All cats in this study were privately owned and examined with the informed consent of their owners. The "Cantonal Committee for Animal Experiments" approved the collection of blood samples (Canton of Bern; permit 71/19).

Informed Consent Statement: The owners of the cats gave written consent to use samples and data for research.

Data Availability Statement: The genome sequence data used in this study are available from the European Nucleotide Archive. Accessions are given in Table S1.

Acknowledgments: The authors are grateful to the cat breeders and owners who donated samples and participated in the study. The authors would like to thank C. Schütz, J. Baskas and P. Grünig for their great technical support and F. Söbbeler for performing the CT and MRI scan. I. Häfliger is acknowledged for helping with variant filtering scripts. We thank the Next Generation Sequencing Platform of the University of Bern for performing the high-throughput sequencing experiments and the Interfaculty Bioinformatics Unit of the University of Bern for providing the high-performance computing infrastructure. The 99 Lives Consortium (Reuben M. Buckley, Danielle Aberdein, Marie Abitbol, Paulo C. Alves, Asa Ohlsson Andersson, Gregory S. Barsh, Rebecca R. Bellone, Tomas F. Bergström, Nuket Bilgen, Adam R. Boyko, Jeffrey A. Brockman, Margret L. Casal, Marta G. Castelhano, Brian W. Davis, Lucy Davison, Ottmar Distl, Nicholas H. Dodman, N. Matthew Ellinwood, Jonathan E. Fogle, Oliver P. Forman, Dorian J. Garrick, Edward I. Ginns, Bianca Haase, Jens Häggström, Robert J. Harvey, Daisuke Hasegawa, Isabel Hernandez, Marjo K. Hytönen, Vidhya Jagannathan, Maria Kaukonen, Christopher B. Kaelin, Tomoki Kosho, Philippa Lait, Emilie Leclerc, Teri L. Lear, Tosso Leeb, Ronald H.L. Li, Hannes Lohi, Maria Longeri, Mark A. Magnuson, Richard Malik, Shrinivasrao P. Mane, Rondo Middleton, John S. Munday, William J. Murphy, Alexandra N. Myers, Niels C. Pedersen, Simon M. Peterson-Jones, Max F. Rothschild, Clare Rusbridge, Jeffrey J. Schoenebeck, Beth Shapiro, Joshua A. Stern, William F. Swanson, Karen A. Terio, Rory J. Todhunter, Wesley C. Warren, Elizabeth A. Wilcox, Julia H. Wildschutte, Yoshihiko Yu, and Leslie A. Lyons) is acknowledged for sharing the cat whole genome sequence data.

Conflicts of Interest: The authors declare no conflict of interest. The funder had no role in the design of the study; in the collection, analyses, or interpretation of data; in the writing of the manuscript, or in the decision to publish the results.

References

1. Krakow, D. Skeletal dysplasias. *Clin. Perinatol.* **2015**, *42*, 301–319. [CrossRef] [PubMed]
2. Mortier, G.R.; Cohn, D.H.; Cormier-Daire, V.; Hall, C.; Krakow, D.; Mundlos, S.; Nishimura, G.; Robertson, S.; Sangiorgi, L.; Savarirayan, R.; et al. Nosology and classification of genetic skeletal disorders: 2019 revision. *Am. J. Med. Genet. Part A* **2019**, *179*, 2393–2419. [CrossRef] [PubMed]
3. Haase, B.; Mazrier, H.; Wade, C.M. Digging for known genetic mutations underlying inherited bone and cartilage characteristics and disorders in the dog and cat. *Vet. Comp. Orthop. Traumatol.* **2016**, *29*, 269–276. [CrossRef] [PubMed]
4. Bannasch, D.L.; Baes, C.F.; Leeb, T. Genetic variants affecting skeletal morphology in domestic dogs. *Trends Genet.* **2020**, *36*, 598–609. [CrossRef] [PubMed]
5. Westworth, D.R.; Sturges, B.K. Congenital spinal malformations in small animals. *Vet. Clin. N. Am. Small Anim Pract.* **2010**, *40*, 951–981. [CrossRef]

6. Takanosu, M.; Takanosu, T.; Suzuki, H.; Suzuki, K. Incomplete dominant osteochondrodysplasia in heterozygous Scottish Fold cats. *J. Small Anim. Pract.* **2008**, *49*, 197–199. [CrossRef] [PubMed]
7. Gandolfi, B.; Alamri, S.; Darby, W.G.; Adhikari, B.; Lattimer, J.C.; Malik, R.; Wade, C.M.; Lyons, L.A.; Cheng, J.; Bateman, J.F.; et al. A dominant TRPV4 variant underlies osteochondrodysplasia in Scottish fold cats. *Osteoarthr. Cartil.* **2016**, *24*, 1441–1450. [CrossRef]
8. Buckley, R.M.; Davis, B.W.; Brashear, W.A.; Farias, F.H.G.; Kuroki, K.; Graves, T.; Hillier, L.W.; Kremitzki, M.; Li, G.; Middleton, R.P.; et al. A new domestic cat genome assembly based on long sequence reads empowers feline genomic medicine and identifies a novel gene for dwarfism. *PLoS Genet.* **2020**, *16*, e1008926. [CrossRef] [PubMed]
9. Struck, A.-K.; Braun, M.; Detering, K.A.; Dziallas, P.; Neßler, J.; Fehr, M.; Metzger, J.; Distl, O. A structural *UGDH* variant associated with standard Munchkin cats. *BMC Genet.* **2020**, *21*, 67. [CrossRef] [PubMed]
10. Lyons, L.A.; Erdman, C.A.; Grahn, R.A.; Hamilton, M.J.; Carter, M.J.; Helps, C.R.; Alhaddad, H.; Gandolfi, B. Aristaless-like homeobox protein 1 (ALX1) variant associated with craniofacial structure and frontonasal dysplasia in Burmese cats. *Dev. Biol.* **2016**, *409*, 451–458. [CrossRef] [PubMed]
11. Lettice, L.A.; Hill, A.E.; Devenney, P.S.; Hill, R.E. Point mutations in a distant sonic hedgehog *cis*-regulator generate a variable regulatory output responsible for preaxial polydactyly. *Hum. Mol. Genet.* **2008**, *17*, 978–985. [CrossRef] [PubMed]
12. Casal, M.L.; Engiles, J.B.; Pipan, M.Z.; Berkowitz, A.; Porat-Mosenco, Y.; Mai, W.; Wurzburg, K.; Xu, M.Q.; Allen, R.; O'Donnell, P.A.; et al. Identification of the identical human mutation in *ACVR1* in 2 cats with fibrodysplasia ossificans progressiva. *Vet. Pathol.* **2019**, *56*, 614–618. [CrossRef]
13. Buckingham, K.J.; McMillin, M.J.; Brassil, M.M.; Shively, K.M.; Magnaye, K.M.; Cortes, A.; Weinmann, A.S.; Lyons, L.A.; Bamshad, M.J. Multiple mutant T alleles cause haploinsufficiency of Brachyury and short tails in Manx cats. *Mamm Genome* **2013**, *24*, 400–408. [CrossRef]
14. Lyons, L.A.; Creighton, E.K.; Alhaddad, H.; Beale, H.C.; Grahn, R.A.; Rah, H.; Maggs, D.J.; Helps, C.R.; Gandolfi, B. Whole genome sequencing in cats, identifies new models for blindness in AIPL1 and somite segmentation in HES7. *BMC Genom.* **2016**, *17*, 265. [CrossRef]
15. Xu, X.; Sun, X.; Hu, X.-S.; Zhuang, Y.; Liu, Y.-C.; Meng, H.; Miao, L.; Yu, H.; Luo, S.-J. Whole Genome Sequencing Identifies a Missense Mutation in HES7 Associated with Short Tails in Asian Domestic Cats. *Sci. Rep.* **2016**, *6*, 31583. [CrossRef] [PubMed]
16. Jagannathan, V.; Drögemüller, C.; Leeb, T.; Dog Biomedical Variant Database Consortium (DBVDC). A comprehensive biomedical variant catalogue based on whole genome sequences of 582 dogs and eight wolves. *Anim. Genet.* **2019**, *50*, 695–704. [CrossRef]
17. Cingolani, P.; Platts, A.; Wang, L.L.; Coon, M.; Nguyen, T.; Wang, L.; Land, S.J.; Lu, X.; Ruden, D.M. A program for annotating and predicting the effects of single nucleotide polymorphisms, SnpEff: SNPs in the genome of Drosophila melanogaster strain w1118; iso-2; iso-3. *Fly* **2012**, *6*, 80–92. [CrossRef]
18. Rusbridge, C.; Knowler, S.P. Hereditary aspects of occipital bone hypoplasia and syringomyelia (Chiari type I malformation) in cavalier King Charles spaniels. *Vet. Rec.* **2003**, *153*, 107–112. [CrossRef] [PubMed]
19. Minato, S.; Baroni, M. Chiari-like malformation in two cats. *J. Small Anim Pract.* **2018**, *59*, 578–582. [CrossRef] [PubMed]
20. Rusbridge, C. New considerations about Chiari-like malformation, syringomyelia and their management. *Practice* **2020**, *42*, 252–267. [CrossRef]
21. Driver, C.J.; Volk, H.A.; Rusbridge, C.; Van Ham, L.M. An update on the pathogenesis of syringomyelia secondary to Chiari-like malformations in dogs. *Vet. J.* **2013**, *198*, 551–559. [CrossRef] [PubMed]
22. Roe, K.A.M.; Syme, H.M.; Brooks, H.W. Congenital large intestinal hypoganglionosis in a domestic shorthair kitten. *J. Feline Med. Surg.* **2010**, *12*, 418–420. [CrossRef] [PubMed]
23. Szylberg, L.; Marszałek, A. Diagnosis of Hirschsprung's disease with particular emphasis on histopathology. A systematic review of current literature. *Prz. Gastroenterol.* **2014**, *9*, 264–269. [CrossRef]
24. Amiel, J.; Lyonnet, S. Hirschsprung disease, associated syndromes, and genetics: A review. *J. Med. Genet.* **2001**, *38*, 729–739. [CrossRef]
25. Jaroy, E.G.; Acosta-Jimenez, L.; Hotta, R.; Goldstein, A.M.; Emblem, R.; Klungland, A.; Ougland, R. "Too much guts and not enough brains": (epi)genetic mechanisms and future therapies of Hirschsprung disease—A review. *Clin. Epigenetics* **2019**, *11*, 1–11. [CrossRef]
26. Gan-Or, Z.; Bouslam, N.; Birouk, N.; Lissouba, A.; Chambers, D.B.; Verlepe, J.; Androschuk, A.; Laurent, S.B.; Rochesfort, D.; Spiegelman, D.; et al. Mutations in CAPN1 cause autosomal-recessive hereditary spastic paraplegia. *Am. J. Hum. Genet.* **2016**, *98*, 1038–1046. [CrossRef]
27. Forman, O.P.; De Risio, L.; Mellersh, C.S. Missense mutation in CAPN1 is associated with spinocerebellar ataxia in the Parson Russell Terrier dog breed. *PLoS ONE* **2013**, *8*, e64627. [CrossRef] [PubMed]
28. Robertson, I.B.; Horiguchi, M.; Zilberberg, L.; Dabovic, B.; Hadjiolova, K.; Rifkin, D.B. Latent TGF-β-binding proteins. *Matrix Biol.* **2015**, *47*, 44–53. [CrossRef] [PubMed]
29. Rifkin, D.B.; Rifkin, W.J.; Zilberberg, L. LTBPs in biology and medicine: LTBP diseases. *Matrix Biol.* **2018**, *71–72*, 90–99. [CrossRef] [PubMed]
30. Koli, K.; Saharinen, J.; Hyytiäinen, M.; Penttinen, C.; Keski-Oja, J. Latency, activation, and binding proteins of TGF-β. *Microsc. Res. Tech.* **2001**, *52*, 354–362. [CrossRef]

31. Chen, Y.; Dabovic, B.; Annes, J.P.; Rifkin, D.B. Latent TGF-β binding protein-3 (LTBP-3) requires binding to TGF-β for secretion. *FEBS Lett.* **2002**, *517*, 277–280. [CrossRef]
32. Zilberberg, L.; Todorovic, V.; Dabovic, B.; Horiguchi, M.; Couroussé, T.; Sakai, L.Y.; Rifkin, D.B. Specificity of latent TGF-β binding protein (LTBP) incorporation into matrix: Role of fibrillins and fibronectin. *J. Cell. Physiol.* **2012**, *227*, 3828–3836. [CrossRef] [PubMed]
33. Koli, K.; Ryynänen, M.J.; Keski-Oja, J. Latent TGF-β binding proteins (LTBPs)-1 and-3 coordinate proliferation and osteogenic differentiation of human mesenchymal stem cells. *Bone* **2008**, *43*, 679–688. [CrossRef] [PubMed]
34. MacFarlane, E.G.; Haupt, J.; Dietz, H.C.; Shore, E.M. TGF-β family signaling in connective tissue and skeletal diseases. *Cold Spring Harb. Perspect. Biol.* **2017**, *9*, a022269. [CrossRef]
35. Noor, A.; Windpassinger, C.; Vitcu, I.; Orlic, M.; Rafiq, M.A.; Khalid, M.; Malik, M.N.; Ayub, M.; Alman, B.; Vincent, J.B. Oligodontia is caused by mutation in LTBP3, the gene encoding latent TGF-β binding protein 3. *Am. J. Hum. Genet.* **2009**, *84*, 519–523. [CrossRef] [PubMed]
36. Huckert, M.; Stoetzel, C.; Morkmued, S.; Laugel-Haushalter, V.; Geoffroy, V.; Muller, J.; Clauss, F.; Prasad, M.K.; Obry, F.; Raymond, J.L.; et al. Mutations in the latent TGF-β binding protein 3 (LTBP3) gene cause brachyolmia with amelogenesis imperfecta. *Hum. Mol. Genet.* **2015**, *24*, 3038–3049. [CrossRef]
37. Dugan, S.L.; Temme, R.T.; Olson, R.A.; Mikhailov, A.; Law, R.; Mahmood, H.; Noor, A.; Vincent, J.B. New recessive truncating mutation in LTBP3 in a family with oligodontia, short stature, and mitral valve prolapse. *Am. J. Med. Genet. Part A* **2015**, *167*, 1396–1399. [CrossRef]
38. Kaur, R.; Siddiqui, I.; Mathur, V.; Jana, M.; Kabra, M.; Gupta, N. Bi-allelic loss-of-function novel variants in LTBP3 -related skeletal dysplasia: Report of first patient from India. *Am. J. Med. Genet. Part A* **2020**, *182*, 1944–1946. [CrossRef]
39. Stanley, S.; Balic, Z.; Hubmacher, D. Acromelic dysplasias: How rare musculoskeletal disorders reveal biological functions of extracellular matrix proteins. *Ann. N. Y. Acad. Sci.* **2021**, *1490*, 57–76. [CrossRef]
40. McInerney-Leo, A.M.; Le Goff, C.; Leo, P.J.; Kenna, T.J.; Keith, P.; Harris, J.E.; Steer, R.; Bole-Feysot, C.; Nitschke, P.; Kielty, C.; et al. Mutations in LTBP3 cause acromicric dysplasia and geleophysic dysplasia. *J. Med. Genet.* **2016**, *53*, 457–464. [CrossRef]
41. Marzin, P.; Thierry, B.; Dancasius, A.; Cavau, A.; Michot, C.; Rondeau, S.; Baujat, G.; Phan, G.; Bonnière, M.; Le Bourgeois, M.; et al. Geleophysic and acromicric dysplasias: Natural history, genotype-phenotype correlations, and management guidelines from 38 cases. *Genet. Med.* **2021**, *23*, 331–340. [CrossRef] [PubMed]
42. Dabovic, B.; Chen, Y.; Colarossi, C.; Zambuto, L.; Obata, H.; Rifkin, D.B. Bone defects in latent TGF-β binding protein (Ltbp)-3 null mice; a role for Ltbp in TGF-β presentation. *J. Endocrinol.* **2002**, *175*, 129–141. [CrossRef]
43. Dabovic, B.; Chen, Y.; Colarossi, C.; Obata, H.; Zambuto, L.; Perle, M.A.; Rifkin, D.B. Bone abnormalities in latent TGF-β binding protein (Ltbp)-3–null mice indicate a role for Ltbp-3 in modulating TGF-β bioavailability. *J. Cell Biol.* **2002**, *156*, 227–232. [CrossRef] [PubMed]
44. Dabovic, B.; Levasseur, R.; Zambuto, L.; Chen, Y.; Karsenty, G.; Rifkin, D.B. Osteopetrosis-like phenotype in latent TGF-β binding protein 3 deficient mice. *Bone* **2005**, *37*, 25–31. [CrossRef] [PubMed]